SCIENCE CHINA
Physics, Mechanics & Astronomy

• Article •
Special Topic: Fluid Mechanics

February 2013 Vol.56 No.2: 263–269
doi: 10.1007/s11433-012-4955-7

Local Reynolds number and thresholds of transition in shear flows

TAO JianJun*, CHEN ShiYi & SU WeiDong

SKLTCS and CAPT, Department of Mechanics and Aerospace Engineering, College of Engineering, Peking University, Beijing 100871, China

Received July 2, 2012; accepted October 25, 2012; published online January 21, 2013

Recent experimental and numerical investigations reveal that the onset of turbulence in plane-Poiseuille flow and plane-Couette flow has some similar stages separated with different threshold Reynolds numbers. Based on these observations and the energy equation of a disturbed fluid element, a local Reynolds number Re_L is derived to represent the maximum ratio of the energy supplement to the energy dissipation in a cross section. It is shown that along the sequence of transition stages, which include transient localized turbulence, "equilibrium" localized turbulence, spatially intermittent but temporally persistent turbulence and uniform turbulence, the corresponding thresholds of Re_L for plane-Couette flow, Hagen-Poiseuille flow and plane-Poiseuille flow are consistent, indicating that the critical (threshold) states during the laminar-turbulent transition are determined by the local properties of the base flow and are independent of global features, such as flow geometries (pipe or channel) and types of driving forces (shear driving or pressure driving).

shear flow, transition, localized turbulence

PACS number(s): 47.20.Ft, 47.20.Pc, 47.27.Cn

Citation: Tao J J, Chen S Y, Su W D. Local Reynolds number and thresholds of transition in shear flows. Sci China-Phys Mech Astron, 2013, 56: 263–269, doi: 10.1007/s11433-012-4955-7

Depending on the amplitude of disturbances, the laminar-turbulent transition in shear flows may have different scenarios. A sequence of bifurcations started with a supercritical instability may occur when the amplitude is small, for example, in Taylor-Couette flows or Rayleigh-Bénard convection [1]. Finite-amplitude disturbances may trigger transitions as well, such as in Hagen-Poiseuille flow and plane-Couette flow, where the base-flow profile is always linearly stable. Recent experiments and numerical simulations have revealed that for the latter type of transition, there are several stages between steady laminar flows and turbulence [2,3]. Shear flows are stable when Reynolds number (Re) is small. $Re = UL/\nu$, where U, L and ν are the characteristic velocity, characteristic length and fluid viscosity of the mean flow, respectively. At small or moderate values of Re, shear flows are always stable to localized disturbances. When Re is larger than a threshold value, say Re_{TLT}, transient and localized turbulence with small scale vortices, such as spots in Couette flow [4–6] and puffs in pipe flow [7–9], can be observed in experiments. When Re is increased further and exceeds another threshold Re_{ELT}, "equilibrium" localized turbulence may appear, e.g., equilibrium puffs in pipe flow [10,11] and turbulent bands in plane-Couette flows. These local coherent structures do not split and remain constant in spatial extent and hence have typical length scales. When Re is large enough (i.e., $Re > Re_{SITP}$), the flow transfers to spatially intermittent but temporally persistent turbulence [12,13]. Finally, uniform turbulence appears when Re is larger than Re_{UT}, and a key feature of uniform turbulence is the Gaussian-type probability distribution function (PDF) of the character disturbing velocity [14]. Different stages in the transition are shown in Figure 1, where the corresponding critical Reynolds numbers are named as well. Since the transition to localized

*Corresponding author (email: jjtao@pku.edu.cn)

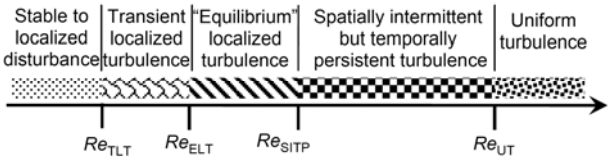

Figure 1 Bifurcation diagram of parallel shear flow.

turbulence occurs when the basic flow is still linearly stable, all the above thresholds can only be observed when the external disturbances are sufficiently strong. The similarities between the transition scenarios of these shear flows suggest that they may follow the same route to turbulence [15], and accordingly a direct quantitative validation of this conjecture is required.

A transition from laminar to turbulent flow is often observed near *Re* of about 2000 for pipe flow and 400 for plane-Couette flow. A readily apparent reason for such discrepancy seems that the Reynolds number is defined with different time and spatial scales for different flows. Consequently, finding a unified control parameter becomes the first and necessary step to understand the universality of transition mechanism. Manneville et al. [16] proposed a "physical Reynolds number" based on the mean shear of basic flow, and it was shown that the corresponding threshold of the banded turbulence pattern [17] in plane-Couette flow coincided with the value of Taylor-Couette flow with zero-average rotation [18–20], but it differed from the thresholds of Poiseuille flows. Since slight local variations in the velocity profile do not cause an apparent change of the mean shear but may lead to instability and trigger the transition in pipe flows [21–24], a unified control parameter should be able to reflect local properties of flow fields.

The velocity profile of steady pipe flow will deviate from the parabolic one for non-Newtonian fluids, and hence may postpone the onset of transition to turbulence. By largely intuitive arguments, Ryan and Johnson [25] used a local control parameter $Z_{\max}$, which represents a ratio of input energy to energy dissipation for an element of fluid, to define the boundary between stable laminar and turbulent flows. It was shown that the critical $Z_{\max}$ of transition obtained in experiments agreed reasonably well between Newtonian fluids and several pseudoplastic fluids moving in straight pipes of circular cross section. In order to avoid the geometry dependence of $Z_{\max}$, Hanks [26] proposed another local parameter κ, which is defined as the ratio of the normal gradient of kinetic energy to the streamwise gradient of pressure. Note that both $Z_{\max}$ and κ are defined with just the properties of steady basic flow and $Z_{\max} = 2\kappa$ for pipe flows. These local parameters have been applied to study the instability and transition of pipe flows for fluid with various suspensions [27], Bingham fluids [28], yield stress fluid and shear thinning fluid [29].

We will derive a local Reynolds number Re_{L} by analyzing the energy equation of a fluid element, and discuss the difference between Re_{L} and the previously defined local parameters. Additionally we will show for the first time that different shear flows have the same thresholds along the sequence of transition stages when Re_{L} is applied.

1 A parameter for fluid element

Since external disturbances cannot be described exactly and completely in advance, most control parameters are defined only based on the base-flow properties. We consider a steady, incompressible and parallel base flow ($U_0(x_2)$, 0, 0). x_1, x_2 and x_3 are the streamwise, normal and spanwise/azimuthal coordinates, respectively. When the flow is perturbed with a disturbance (u, v, w), the governing equations of motion for a fluid element can be written as:

$$\rho \frac{\mathrm{d}U_i}{\mathrm{d}t} = \frac{\partial \sigma_{ij}}{\partial x_j}, \quad i, j = 1, 2, 3, \tag{1}$$

where $U_1=U_0+u$, $U_2=v$, $U_3=w$, $\sigma_{ij} = \sigma_{0,ij} + \tau_{ij}$. σ_{ij} and τ_{ij} indicate the total and disturbing stress components exerted in the x_i direction at the element surface normal to x_j. The subscript $_0$ represents the base-flow properties and $\partial \sigma_{0,ij} / \partial x_j = 0$ because the base flow is steady. An energy equation can be obtained by taking the scalar product of eq. (1) and the vector velocity of the base flow,

$$\frac{\rho}{2} \frac{\mathrm{d}(U_0 U_1)}{\mathrm{d}t} = \frac{\rho v U_1}{2} \frac{\mathrm{d}U_0}{\mathrm{d}x_2} + \frac{U_0}{2} \frac{\partial \tau_{1i}}{\partial x_i}. \tag{2}$$

Since $v^2 \ll U_0 U_1$, $w^2 \ll U_0 U_1$ and $U_0 U_1 \approx U_1^2$, the term on the left side of eq. (2) is an estimation of the growth rate, unit-volume basis, of total kinetic energy in a disturbed fluid element. On the right side, the first term represents the rate of energy supplement transferred from the main stream, and the remaining term represents the rate of energy dissipation. The energy ratio α is

$$\alpha = \rho v U_1 \frac{\mathrm{d}U_0}{\mathrm{d}x_2} \Bigg/ \left(U_0 \frac{\partial \tau_{1i}}{\partial x_i} \right) \approx \rho v \left(\frac{\mathrm{d}U_0}{\mathrm{d}x_2} \Bigg/ \frac{\partial \tau_{1i}}{\partial x_i} \right). \tag{3}$$

In order to define a nondimensional control parameter to describe the most vulnerable state to external perturbations, we examine the largest energy ratio α in a cross section when fluid elements are exerted with the same disturbing force per unit volume as that at the wall $F=\rho\, \mathrm{d}u/\mathrm{d}t=\rho \mathrm{d}U_1/\mathrm{d}t=\partial \tau_{1i} / \partial x_i = (\partial \tau_{1i} / \partial x_i)_{\mathrm{wall}}$.

To carry this analysis further one would need to define the form of the perturbation stream function, which is not known in most realistic cases, and one thus would lose generality. Eckhardt [2] and Manneville [3] have summarized several well-defined thresholds (lower bounds) during the transition to turbulence for both channel and pipe flows

when the perturbations are strong enough. Based on these observations, it is postulated that at these critical states the characteristic time scale of effective disturbances is related to the corresponding value of the base flow, namely,

$$\rho\left|v\Big/\left(\frac{\partial\tau_{1i}}{\partial x_i}\right)_{\text{wall}}\right| = C\rho\left|U_0\Big/\frac{\tau_{0,\text{w}}}{R_\text{h}}\right|, \tag{4}$$

where C is a coefficient and may be different at different critical (threshold) states. $\tau_{0,\text{w}}$ is the wall shear stress of the base flow and R_h is the corresponding hydraulic radius, which is widely used to assess different channels' transport capacity in hydraulic engineering,

$$R_\text{h} = \frac{\text{the cross-sectional area of flow}}{\text{wetted perimeter}}. \tag{5}$$

It can be verified that R_h is half the height h of a parallel-plate channel with infinite width and $R_\text{h}=R/2$ for straight pipe with circular section. Here R is the radius of the pipe. Consequently, the maximum ratio of the energy supplement to the energy dissipation (eq. (3)) in the normal direction $\alpha_{\max}$ can be evaluated with the base-flow properties as:

$$\begin{aligned}\alpha_{\max} &= \left|\rho\nu U_1\frac{\text{d}U_0}{\text{d}x_2}\Big/\left(U_0\frac{\partial\tau_{1i}}{\partial x_i}\right)\right|_{\max}\\ &\approx C\left|\rho R_\text{h}U_0\frac{\text{d}U_0}{\text{d}x_2}\Big/\tau_{0,\text{w}}\right|_{\max} = CRe_\text{L}.\end{aligned} \tag{6}$$

Since C is a constant coefficient, the local Reynolds number Re_L represents the maximum energy rate of a fluid element at the critical (threshold) state. Considering that Re_L is derived directly from the energy equation without specifying the base-flow geometry or the type of driving force (e.g., pressure-driving or shear driving), physically it is a generalized control parameter for viscous shear flow.

In order to verify the universality of transition scenario, this local parameter is applied to three types of shear flows, namely the Hagen-Poiseuille flow, plane-Poiseuille flow and plane-Couette flow. The coordinates are laid at the axis of pipe and the middle plane of channels, respectively. For Hagen-Poiseuille flow, by substituting basic flow solution $U_0 = U_\text{M}(1-r^2/R^2)$ into eq. (6) we find that $Re_\text{L} = U_\text{M}R\big/(3\sqrt{3}\nu)$ at $r=R/\sqrt{3}$. Similarly, for plane-Poiseuille flow $U_0 = U_\text{M}(1-y^2/h^2)$, we can obtain $Re_\text{L}=2Re/3\sqrt{3}$. U_M is the maximum velocity of the cross section. For plane-Couette flow $U_0 = U_\text{M}y/h$, the local Reynolds number Re_L is just the same as the classical one.

Based on a linearized two-dimensional energy equation, Ryan and Johnson [25] proposed a local parameter $Z_{\max}$ to describe the transition threshold of non-Newtonian fluids in pipe flows. Hanks [26] extended the concept to plane-Poiseuille flow and suggested another locally defined control parameterκ, which is equivalent to $Z_{\max}$ for pipe flow ($Z_{\max}=2\kappa$).

$$Z_{\max} = \sqrt{\frac{4}{27}}\frac{RU_\text{M}}{\nu},\quad \kappa = \frac{1}{2}\rho\left|\frac{\nabla(U_0^2)}{\nabla p_0}\right|_{\max},$$

where the subscript "max" means the maximum value in the cross section. The definitions of three local parameters are shown in Table 1 for different shear flows. Note that κ cannot be applied to shear-driven flows, e.g., Couette flow where $\nabla p_0 = 0$. For Hagen-Poiseuille flow, $Z_{\max}=2Re_\text{L}$ and the factor 2 is caused by the fact that we use a generalized length scale (eq. (5)) in this paper. Therefore, comparing with $Z_{\max}$ and κ, Re_L is a more generalized control parameter.

As a reference, the Reynolds number defined with mean shear is derived as well,

$$\overline{Re} = \frac{(\text{mean shear})(\text{characteristic length } L)^2}{\nu}.$$

For plane-Couette flow, experiments show that streamwise vortices and streaks, which are the dominant structures in the transition range, develop in the full gap, hence $L=2h$ and $\overline{Re}=(U_\text{M}/h)(2h)^2/\nu=4Re$. If the plane-Poiseuille flow can be understood as two plane-Couette flows side by side each of width h and velocity difference U_M, and at the moderate Reynolds numbers of interest disturbance structures developing in one half of the system are relatively independent of what happens in the other, then L is set to h and $\overline{Re}=(U_\text{M}/h)h^2/\nu=Re$. For Hagen-Poiseuille flow, the mean shear is of the order of U_M/R and thus $\overline{Re}=(U_\text{M}/R)R^2/\nu=Re$.

2 Results and discussion

The traditional Re only includes the global scales of the mean flow, hence cannot distinguish between plane-Couette flow and plane-Poiseuille flow with the same channel height and the same maximum velocity. It is shown in sect. 1 that the mechanism governing the growth of kinetic energy of a fluid element is the same for different shear flows, hence Re_L, defined with terms including local time and spatial sca-

Table 1 Definitions of Re, $Z_{\max}$, κ, $\overline{Re}$ and Re_L. h is the half height between the two plates, R is the radius of the pipe and U_M is the maximum velocity of the base flow. PCF, HPF and PPF represent the plane-Couette flow, Hagen-Poiseuille flow and plane-Poiseuille flow, respectively

Flow type	Re	$Z_{\max}$	κ	$\overline{Re}$	Re_L
PCF	$\frac{U_\text{M}h}{\nu}$	–	–	$\frac{4U_\text{M}h}{\nu}$	$\frac{U_\text{M}h}{\nu}$
HPF	$\frac{U_\text{M}R}{\nu}$	$\frac{2}{3\sqrt{3}}\frac{U_\text{M}R}{\nu}$	$\frac{1}{3\sqrt{3}}\frac{U_\text{M}R}{\nu}$	$\frac{U_\text{M}R}{\nu}$	$\frac{1}{3\sqrt{3}}\frac{U_\text{M}R}{\nu}$
PPF	$\frac{U_\text{M}h}{\nu}$	–	$\frac{2}{3\sqrt{3}}\frac{U_\text{M}h}{\nu}$	$\frac{U_\text{M}h}{\nu}$	$\frac{2}{3\sqrt{3}}\frac{U_\text{M}h}{\nu}$

les (e.g., $dU_0(x_2)/dx_2$ in eq. (6)), is expected to be able to mark the universality of transition stages.

2.1 Plane-Couette flow

Plane-Couette flow represents the simplest solution of the Navier-Stokes equation of motion, and turbulence was observed experimentally when Re>280 [30]. By introducing a thin wire parallel to the spanwise direction in the center plane, Bottin et al. [31] found that transient localized turbulence started to be formed at Re = 290, and this critical value is confirmed later by numerical simulations [32]. Eckhardt et al. [33] studied numerically the initial stage of transition, and observed that the probability of finding long-lived transient states for repeated calculations started to deviate from zero at Re = 280–290. Therefore, Re_{TLT} defining the initial appearance of transient localized turbulence is around 290.

An early experimental study found a critical Reynolds number for a self-sustaining spot as Re = 370 ± 10 [4], and a later experiment estimated it as Re = 325 ± 5 [6]. For 340 <Re<394 (see ref. [17], Figure 2(b)) a spatially periodic pattern composed of distinct regions of turbulent and laminar flow has been discovered in plane-Couette experiments. Since the turbulent stripes are statistically stationary and are isolated periodically by laminar bands with well-defined wavelength and tilt angle, they are referred to as "equilibrium" localized turbulence in this paper. Barkley and Tuckerman [32] reported the first direct numerical simulation of turbulent-laminar patterns. They found that at Re = 390 stable pattern formed with distinct turbulent and laminar regions while at Re = 400 the flow became spatially intermittent-quasilaminar regions nucleated and disappeared continually. By direct numerical simulations in a very large domain Duguet et al. [12] observed that a pattern consisted of alternating laminar and turbulent bands would fill up the whole numerical domain at 330⩽Re⩽380.

It is also found that with the increase of Re turbulent stripes still emerged eventually, but became less well-defined. When Re is approximately 400 the laminar zones emerge spontaneously and transiently, hence the flow becomes spatially intermittent, though the turbulent area fraction remains almost time independent. When Re is increased further, the flow may turn to be uniform turbulence. Recently, Tuckerman et al. [34] have shown that the PDF of the characteristic disturbing velocity was almost identical to a Gaussian type for 500⩽Re⩽600, and the fitting coefficients of a quartic polynomial proposed for the PDF changed very little for Re>500 (see ref. [14], Figure 8). Based on the above experimental and numerical results, it can be concluded that the thresholds for the "equilibrium" localized turbulence, the spatially intermittent but temporally persistent turbulence and the uniform turbulence are $Re_{ELT} \simeq 330$, $Re_{SITP} \simeq 390$ and Re_{UT} = 500, respectively.

2.2 Hagen-Poiseuille flow

After introducing a jet at an upstream position in a pipe, localized turbulent structures bounded by regions of laminar flow, the reputed puffs [7], are recorded downstream when Re increases to 1500 [35]. Peixinho and Mullin [36] performed a series of experiments with different types of disturbances and perturbation amplitudes. They found that the critical Reynolds number, where localized turbulence starts to be formed, decreased with the increase of the disturbance amplitude until a lower threshold is reached. The bottom error bars for single jet disturbances and for spanwise push-pull disturbances (see ref. [36], Figures 3 and 4) indicate a rapid decay of disturbances and their averaged value 1513 is referred as the threshold Re_{TLT}, which is close to Hof et al. [35] observations. At higher Reynolds numbers, a meta-stable state or the reputed "equilibrium" puff [10,11], that is, one which does not grow, split or shrink (statistically 20 diameters long) as it travels through a long pipe. By injecting perturbations into the pipe flow and observing their decay, Darbyshire and Mullin [8] summarized their experiments and concluded that the critical threshold of turbulent structures was in the range of $Re \approx 1760$, below which no sustained turbulence was observed. Peixinho and Mullin [36] investigated the relaminarization of puffs and found that with the increase of Re, the time required for puffs to decay increased sharply at Re = 1750±10. Such critical behavior was qualitatively supported by a numerical investigation [37], though the extrapolated critical Reynolds number 1870 was larger than the experimental value.

In addition, recent numerical and experimental studies [36–40] all support a paradigm that the transition to turbulence in pipe flow is linked to a strange saddle in the phase space of the Navier-Stokes equations [15], and the turbulent lifetimes, the time prior to escaping the saddle, are exponentially distributed. By using substantially larger sample size of simulations than previously used, Avila et al. [41] studied the lifetime data and showed that the lifetimes are not exponentially distributed until $Re \approx 1720$. This result suggests the existence of a saddle-node bifurcation and hence the corresponding threshold for "equilibrium" puff is set as $Re_{ELT} \approx 1720$.

Although it is shown that every single puff has finite lifetime [42], Wygnanski et al. [10] and Nishi et al. [43] showed that they could split at higher Reynolds numbers. More recently, Avila et al. [13] illustrate numerically and experimentally that with increasing Reynolds number the mean lifetime of puffs increases rapidly, while the mean time it takes for them to split decreases. At Re = 2040 ± 10 these two characteristic time coincides with each other, and accordingly the flow turn to be spatially intermittent while the turbulent fraction is temporally persistent, namely Re_{SITP} = 2040±10. Based on experimental observations, Patel and Head [44] suggested that intermittency disappeared when the Reynolds number Re is in the region of 3000. By sys-

tematically analyzing the numerical results of the transition between intermittent and uniform turbulence, Moxey and Barkley [11] defined a critical Reynolds number for uniform turbulence ($Re_{UT} \simeq 2600$) along the pipe, where the PDF of the characteristic disturbing velocity was close to a Gaussian type.

2.3 Plane-Poiseuille flow

In the first flow visualization study of spots in plane-Poiseuille flow, Carlson et al. [45] summarized that below a Reynolds number (defined with h and centerline velocity) of about 840 a disturbance was found to grow into a semi-developed spot and then decay into a streamwise structure that ultimately disappeared. Therefore, the threshold for equilibrium spot satisfied $Re_{ELT} \geqslant 840$. At a Reynolds number of about 1000, a strong, repeatable, growing spot could be triggered and spot-splitting, the counterpart of puff-splitting in pipe flow, might occur as the spot moved downstream (see ref. [45], Figure 6). Hence the critical value for spatially intermittent but temporally persistent turbulence satisfies $Re_{SITP} \simeq 1000$. In a later experiment [46], turbulent spots could not be generated for $Re<1100$. We have done direct numerical simulations in a periodic domain of $160h \times 2h \times 120h$ ($768 \times 65 \times 1024$ grids system). The growth of spots and spot-splitting are observed at $Re = 1000$ and hence our DNS results are consistent with Carlson's observations. At higher Reynolds number, Patel and Head [44] concluded that the uniform turbulence or disappearance of intermittency was first observed experimentally at $2h\bar{U}_0/\nu \simeq 1800$ or $Re \simeq 1350$, where $\bar{U}_0$ is the mean (bulk) velocity. Recently, turbulent stripes are still observed experimentally and numerically at $2h\bar{U}_0/\nu$=2000 [47]. Since we focus on the lower bound of every transition stage, the threshold of uniform turbulence is estimated as $Re_{UT} \simeq 1350$.

Four transition thresholds discussed above for plane-Couette flow, plane-Poiseuille flow and Hagen-Poiseuille flow are summarized in Table 2. It can be seen clearly that the traditional Reynolds number thresholds differ significantly between these flows, and $\overline{Re}$ thresholds show a better agreement than Re with a relative difference about 35%–110%. When the local Reynolds number Re_L is applied, the series of threshold values for different shear flows, from the onset of transient localized turbulence to uniform turbulence, almost coincide with each other and have a percentage difference less than 5%. These unified thresholds confirm quantitatively the intrinsic consistency and determinacy of the transition process.

It should be noted that the unified milestones along the route to turbulence do not suggest that the whole transition scenarios can be transformed completely from one flow to another. The reasons are as follows. Firstly, we only compare the lower band of every transition stage, which is unique for every kind of flow and hence the corresponding effective disturbance has strong correlation with the base-flow solution as described by eq. (4). Between these thresholds, e.g., $Re_{TLT}<Re<Re_{ELT}$, the critical Reynolds number of localized turbulence is determined not only by the base-flow information but also by the style and amplitude of disturbances as shown by previous experiments [36]. Secondly, though the sustaining mechanism of disturbances is universal as described by eq. (2), their long-term evolution may be different because of boundary conditions in different shear flows. For example, the "equilibrium" localized turbulence has typical streamwise and spanwise length scales L_{st} and L_{sp}, whose corresponding values for plane-Couette flow, plane-Poiseuille flow and Hagen-Poiseuille flow are (L_{st}; L_{sp}) $\approx$ ($110h$; $50h$–$80h$) at $340 \leqslant Re \leqslant 395$ [18], ($40h$; $30h$) at $Re = 1000$ [45] and ($40R$; $<2R$) [48], respectively. It is readily apparent that the L_{sp} of Hagen-Poiseuille flow is one-order smaller than those of channel flows due to the spanwise confinement. Considering that energy dissipation of turbulence is mostly contributed by fine flow structures, pipe flows will have larger percentage of energy dissipated by disturbances with small spanwise (or azimuthal) length scales than channel flows. Though such extra energy dissipation is small and does not affect the transition thresholds, it accumulates along with the downstream advection and may lead to the eventual decay of puffs. These intuitive arguments explain to some degree a discrepancy between pipe flows and channel flows, namely, when $Re > Re_{ELT}$ the turbulent bands or spots in channel flows can sustain and behave as chaotic attractors [12,45], while the "equilibrium"

Table 2 Comparison of the threshold Reynolds numbers during the laminar-turbulent transition

Flow type	Re_{TLT}	$\overline{Re}$	Re_L
Plane-Couette	280	1120	280
	290	1160	290
	290	1160	290
	280–290	1120–1160	280–290
Hagen -Poiseuille	1500	1500	288.6
	1513	1513	291.1
	Re_{ELT}		
Plane-Couette	340	1360	340
	325±5	1300±20	325±5
	330	1320	330
Hagen-Poiseuille	1760	1760	338.6
	1750±10	1750±10	336.7±1.9
	1720	1720	331
Plane-Poiseuille	$\geqslant$840	$\geqslant$840	323.3
	Re_{SITP}		
Plane-Couette	394	1576	394
	390–400	1560–1600	390–400
	380–400	1520–1600	380–400
Hagen-Poiseuille	2040±10	2040±10	392.5±1.9
Plane-Poiseuille	$\simeq$ 1000	$\simeq$ 1000	$\simeq$ 385
	Re_{UT}		
Plane-Couette	500	2000	500
	500	2000	500
Hagen-Poiseuille	2600	2600	500.4
Plane-Poiseuille	$\simeq$ 1350	$\simeq$ 1350	$\simeq$ 519.6

puffs in pipe flow are meta-stable transients [41,42,49] and behave as strange repellers.

3 Conclusions

Recent numerical and experimental progresses on localized turbulence in shear flows make it possible to compare their routes to turbulence quantitatively. As a first step, a unified control parameter—local Reynolds number Re_L is derived based on the energy equation of a fluid element. The available numerical and experimental data are analyzed and the transition route is divided into several stages, the transient localized turbulence, the "equilibrium" localized turbulence, the spatially intermittent but temporally persistent turbulence and uniform turbulence. It is shown that the corresponding Re_L thresholds for plane-Couette flow, plane-Poiseuille flow and Hagen-Poiseuille flow are consistent with each other. This surprising agreement indicates that it is the local properties, not global characteristics (e.g., flow geometries or types of driving forces) of a base flow that determine the key features of the transition scenario. The unified thresholds are sufficiently well-defined to await further calibrations with other viscous shear flows.

We thank BUSSE F H, TUCKERMAN L, MANNEVILLE P, ECKHARDT B, DUGUET Y, AVILA M, NAGATA M, HOF B and DOU H for insightful discussions regarding transition in shear flows. This work was supported by the National Natural Science Foundation of China (Grant Nos. 10972007 and 10921202) and (Grant No. 2009CB724100).

1 Busse F H. The sequence-of-bifurcations approach towards understanding turbulent fluid flow. Surv Geophys, 2003, 24: 269–288
2 Eckhardt B. A critical point for turbulence. Science, 2011, 333: 165–166
3 Manneville P. Understanding the sub-critical transition to turbulence in wall flows. PRAMANA. J Phys, 2008, 70: 1009–1021
4 Daviaud F, Hegseth J, Berg P. Subcritical transition to turbulence in plane Couette flow. Phys Rev Lett, 1992, 69: 2511–2516
5 Tillmark N, Alfredsson P H. Experiments on transition in plane Couette flow. J Fluid Mech, 1992, 235: 89–102
6 Dauchot O, Daviaud F. Finite amplitude perturbation and spots growth mechanism in plane Couette flow. Phys Fluids, 1995, 7: 335–343
7 Wygnanski I J, Champagne F H. On transition in a pipe. Part 1. The origin of puffs and slugs and the flow in a turbulent slug. J Fluid Mech, 1973, 59: 281–335
8 Darbyshire A G, Mullin T. Transition to turbulence in constant-mass-flux pipe flow. J Fluid Mech, 1995, 289: 83–114
9 Eckhardt B, Schneider T M, Hof B, et al. Turbulence transition in pipe flow. Annu Rev Fluid Mech, 2007, 39: 447–468
10 Wygnanski I J, Sokolov M, Friedman D. On transition in a pipe. Part 2. The equilibrium puff. J Fluid Mech, 1975, 69: 283–304
11 Moxey D, Barkley D. Distinct large-scale turbulent-laminar states in transitional pipe flow. Proc Natl Acad Sci USA, 2010, 107: 8091–8096
12 Duguet Y, Schlatter P, Henningson D S. Formation of turbulent patterns near the onset of transition in plane Couette flow. J Fluid Mech, 2010, 650: 119–129
13 Avila K, Moxey D, de Lozar A, et al. The onset of turbulence in pipe flow. Science, 2011, 333: 192–196
14 Tuckerman L S, Barkley D. Patterns and dynamics in transitional plane Couette flow. Phys Fluids, 2011, 23: 041301
15 Eckhardt B. Turbulence transition in pipe flow: Some open questions. Nonlinearity, 2008, 21: T1–T11
16 Manneville P, Prigent A, Dauchot O. Banded turbulence in Taylor-Couette and plane Couette flow. APS/DFD meeting. Bull Am Phys Soc, 2001, 46: 35
17 Prigent A, Grégoire G, Chaté H, et al. Large-scale finite-wavelength modulation within turbulent shear flows. Phys Rev Lett, 2002, 89: 014501
18 Prigent A, Grégoire G, Chaté H, et al. Long-wavelength modulation of turbulent shear flows. Phys D, 2003, 174: 100–113
19 Manneville P. Spots and turbulent domains in a model of transitional plane Couette flow. Theor Comput Fluid Dyn, 2004, 18: 169–181
20 Barkley D, Tuckerman L S. Mean flow of turbulent-laminar patterns in plane Couette flow. J Fluid Mech, 2007, 576: 109–137
21 Gill A E. A mechanism for instability of plane Couette flow and of Poiseuille flow in a pipe. J Fluid Mech, 1965, 21: 503–511
22 Gavarini M I, Bottaro A, Nieuwstadt F T M. The initial stage of transition in pipe flow: Role of optimal base-flow distortions. J Fluid Mech, 2004, 517: 131–165
23 Ben-Dov G, Cohen J. Critical Reynolds number for a natural transition to turbulence in pipe flows. Phys Rev Lett, 2007, 98: 064503
24 Tao J. Critical instability and friction scaling of fluid flows through pipes with rough inner surfaces. Phys Rev Lett, 2009, 103: 264502
25 Ryan N W, Johnson M. Transition from laminar to turbulent flow in pipes. AICHE J, 1959, 5: 433–435
26 Hanks R W. The laminar-turbulent transition for flow in pipe, concentric annuli, and parallel plates. AICHE J, 1963, 9: 45–48
27 Fur B Le, Martin M. Laminar and transitional flow of drilling muds and various suspensions in circular tubes. J Fluid Mech, 1967, 30: 449–463
28 Nouar C, Frigaard I A. Nonlinear stability of Poiseuille flow of a Bingham fluid: Theoretical results and comparison with phenomenological criteria. J Non-Newtonian Fluid Mech, 2001, 100: 127–149
29 Peixinho J, Nouar C, Desaubry C, et al. Laminar transition and turbulent flow of yield stress fluid in a pipe. J Non-Newtonian Fluid Mech, 2005, 128: 172–184
30 Leutheusser H J, Chu V H. Experiments on plane Couette flow. J Hyd Div Am Sot Civ Eng, 1971, 97: 1269–1284
31 Bottin S, Dauchot O, Daviaud F. Intermittency in a locally forced plane Couette flow. Phys Rev Lett, 1997, 79: 4377–4380
32 Barkley D, Tuckerman L S. Computational study of turbulent laminar patterns in Couette flow. Phys Rev Lett, 2005, 94: 014502
33 Eckhardt B, Faisst H, Schmiegel A, et al. Dynamical systems and the transition to turbulence in linearly stable shear flows. Phil Trans R Soc A, 2008, 366: 1297–1315
34 Tuckerman L S, Barkley D, Moxey O, et al. Order parameter in laminar-turbulent patterns. In: Eckhardt B, ed. Advances in Turbulence XII. NY: Springer, 2009. 132: 89–91
35 Hof B, van Doorne C W H, Westerweel J, et al. Turbulence regeneration in pipe flow at moderate Reynolds numbers. Phys Rev Lett, 2005, 95: 214502
36 Peixinho J, Mullin T. Finite-amplitude thresholds for transition in pipe flow. J Fluid Mech, 2007, 582: 169–178
37 Willis A P, Kerswell R R. Critical behavior in the relaminarization of localized turbulence in pipe flow. Phys Rev Lett, 2007, 98: 014501
38 Faisst H, Eckhardt B. Sensitive dependence on initial conditions in transition to turbulence in pipe flow. J Fluid Mech, 2004, 504: 343–352
39 Hof B, Westerweel J, Schneider T M, et al. Finite lifetime of turbulence in shear flows. Nature, 2006, 443: 59–62
40 Peixinho J, Mullin T. Decay of turbulence in pipe flow. Phys Rev Lett, 2006, 96: 094501

41 Avila M, Willis A P, Hof B. On the transient nature of localized pipe flow turbulence. J Fluid Mech, 2010, 646: 127–136
42 Hof B, de Lozar A, Kuik D J, et al. Repeller or attractor? Selecting the dynamical model for the onset of turbulence in pipe flow. Phys Rev Lett, 2008, 101: 214501
43 Nishi M, Ünsal B, Durst F, et al. Laminar-to-turbulent transition of pipe flows through puffs and slugs. J Fluid Mech, 2008, 614: 425–446
44 Patel V C, Head M R. Some observations on skin friction and velocity profiles in fully developed pipe and channel flows. J Fluid Mech, 1969, 38: 181–201
45 Carlson D R, Widnall S E, Peeters M F. A flow-visualization study of transition in plane Poiseuille flow. J Fluid Mech, 1982, 121: 487–505
46 Alavyoon F, Henningson D S, Alfredsson P H. Turbulent spots in plane Poiseuille flow-flow visualization. Phys Fluids, 1986, 29: 1328–1331
47 Tsukahara T, Kawaguchi Y, Kawamura H, et al. Turbulence stripe in transitional channel flow with/without system rotation. IUTAM Book Ser, 2010, 18: 421–426
48 Mullin T. Experimental studies of transition to turbulence in a pipe. Annu Rev Fluid Mech, 2011, 43: 1–24
49 Kuik D J, Poelma C, Westerweel J. Quantitative measurement of the lifetime of localized turbulence in pipe flow. J Fluid Mech, 2010, 645: 529–539